NORTH CAROLINA

A & T STATE UNIVERSITY

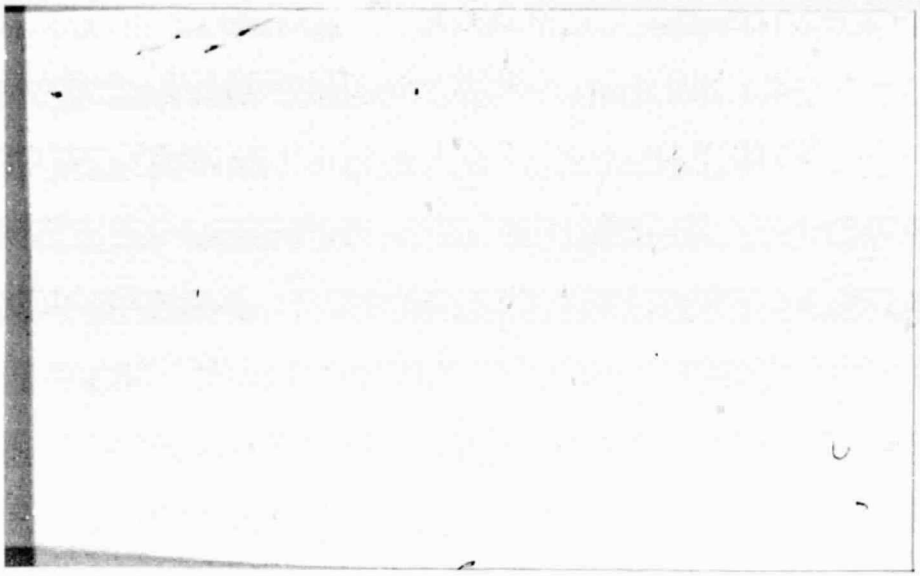

SCHOOL OF ENGINEERING

DEPARTMENT OF MECHANICAL ENGINEERING

GREENSBORO, N.C. 27411

FINAL REPORT

EFFECT OF TEMPERATURE ON COMPOSITE SANDWICH STRUCTURES SUBJECTED TO LOW VELOCITY IMPACT

Avva V. Sharma
Professor of Mechanical Engineering

NSG-1296 1976-79

Prepared for

Langley Research Center
National Aeronautics and Space Administration
Technical Officer: Marvin D. Rhodes

School of Engineering
North Carolina A. and T. State University
Greensboro, North Carolina

February 1980

ACKNOWLEDGMENTS

The financial support provided for this work by the National Aeronautics and Space Administration through a grant NSG-1296 is gratefully acknowledged. The author is grateful to Dr. Martin Mikulas of the Langley Research Center for his interest and encouragement during the initial phase of this investigation. Further, the author extends his sincere appreciation to Mr. Marvin D. Rhodes, Technical Officer, for his assistance in the experimental arrangement and for rendering many valuable suggestions during the course of this investigation.

EFFECT OF TEMPERATURE ON COMPOSITE SANDWICH STRUCTURES
SUBJECTED TO LOW VELOCITY IMPACT

ABSTRACT

An experimental investigation was conducted to study the effect of low velocity projectile impact on sandwich-type structural components. The materials used in the fabrication of the impact surface were graphite-, Kevlar-, and boron-fibers with appropriate epoxy matrices. The testing of the specimens was performed at moderately low- and high-temperatures as well as at room temperature to assess the impact-initiated strength degradation of the laminates. Eleven laminates with different stacking sequences, orientations, and thicknesses were tested. The low energy projectile impact is considered to simulate the damage caused by runway debris, the dropping of the hand tools during servicing, etc., on the secondary aircraft structures fabricated with the composite materials. The results show the preload and the impact energy combinations necessary to cause catastrophic failures in the laminates tested. A set of faired curves indicating the failure thresholds is shown separately for the tension- and compression-loaded laminates. The specific-strengths and -modulii for the various laminates tested are also given.

TABLE OF CONTENTS

LIST OF TABLES

LIST OF FIGURES

INTRODUCTION

The use of graphite/epoxy composites and composites fabricated out of similar fibrous materials in the design of secondary structural components of aircraft is gaining momentum in recent years. Some of these components are designed with a honeycomb type core between the composite facings. In the normal operational mode, these components may be exposed to foreign object damage such as the dropping of hand tools, runway debris, etc., resulting in the loss of the composite strength. Consequently, it is of interest to study the impact-related damage caused by foreign objects and to develop design criteria in the use of composite sandwich structures. Several studies on the laminated composites were conducted by Slepetz (1)*, et al., Rhodes (2,3,4), Awerbuck and Hahn (5), and Sharma (6-9). The impact damage tolerance of composites such as graphite/epoxy, graphite/S-glass, boron/aluminum, borsic/titanium, Kevlar-graphite/epoxy and boron-graphite/epoxy was evaluated in the above studies. Some of these studies were concerned with visible surface damage evaluation. Rhodes (3,4) studied the effect of the projectile impact on the strength carrying capacity of the composite sandwich structures. Some of the variables in the studies by Rhodes were laminate orientation, stacking sequence, and thickness. These studies were conducted at room temperature to observe the visual damage- and failure-thresholds of composites under low velocity impact. The studies conducted by Sharma (6-9) were similar in scope to that of Rhodes. The results reported by Sharma (7) were concerned with the effect of moderately high- and low-temperatures on the load carrying ability of some of the composites tested. These results were compared with the corresponding results obtained at room temperature by Rhodes (4). Some of the results reported by Sharma (6,8,9) were based on room temperature studies on the composite laminates having various combinations of plies, fibers, matrices, and stacking sequences.

The objective of the present report is to analyze all the data reported in the previous presentations (6-9) and to present a comprehensive comparative study of all laminates tested by the author.

*Numbers in the parer theses designate reference at the end of the report.

SPECIMENS AND EXPERIMENTAL ARRANGEMENT

Eleven different specimen configurations were evaluated in this investigation (Table I). Each lamina in the panel had a nominal cured thickness of 140 x 10^{-6} m (0.0055 in.). The honeycomb sandwich specimens were fabricated using the composite laminate as the face sheet (test surface) and a steel plate as the back surface. The nominal dimensions of the specimen were 56 cm (22 in.) long by 7.5 cm (3 in.) wide with a honeycomb core thickness of 2.5 cm (1 in.). The area of the core in the center test section, where a uniform stress field was imposed through a four-point loading apparatus, was 7.5 (3 in.) by 7.5 cm (3 in.). All specimens except Series 7 had a 0.32 cm (1/8 in.) cell; 130 kg/m^3 (8.1 lbm/ft^3) aluminum honeycomb core in the test section. The Series 7 had a 0.32 cm (1/8 in.) cell, 48 kg/m^3 (3.0 lbm/ft^3) Nomex honeycomb core. A dense aluminum core was used in the end sections of the beam where high shear loads exist. Large face panels were laid at predetermined ply-orientations and cured. These cured panels were cut to size and bonded adhesively to the core material. The subscripts B, G, and K in the laminate orientation code refer to boron, graphite, and Kevlar, respectively.

A schematic diagram of the projectile firing mechanism is shown in Figure 1. Air is bled from a supply line into a cylindrical reservoir until the one-mil-thick mylar diagram ruptures. The air escapes through a tiny hole - the size of which was predetermined based on a desired projectile velocity - located in the center of the orifice plate and propels the projectile toward the specimen through a gun barrel. The projectile is an aluminum sphere 1.27 cm (0.5 in.) in diameter. A velocity measuring device is located in front of the test specimen. As the projectile travels through this device, light beams emitted by photodiodes are interrupted and an electronic counter is triggered. The average velocity of the projectile is calculated from the distance between the photodiodes and the time required by the projectile to traverse this distance.

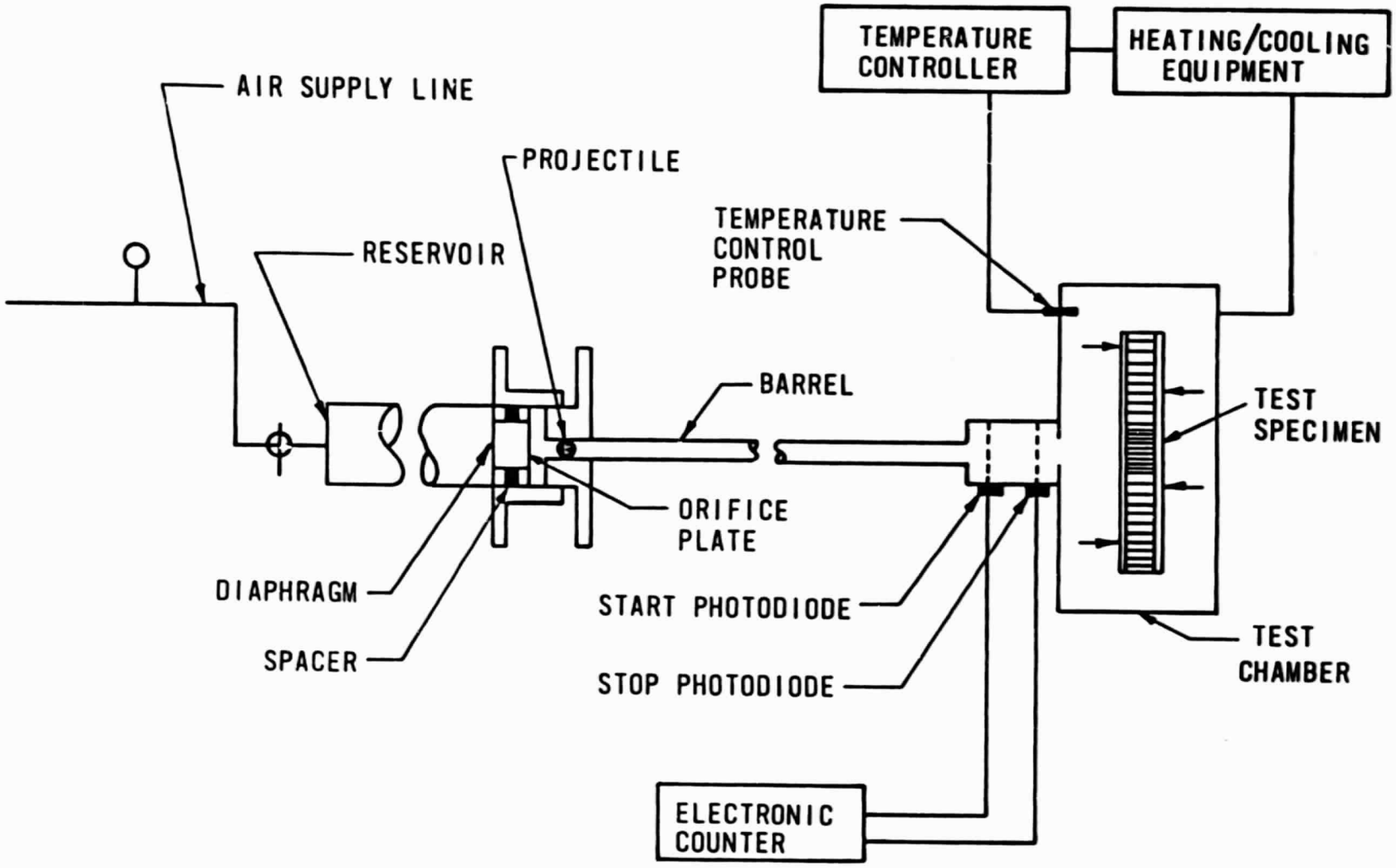

Figure 1. Schematic Diagram of Firing Mechanism.

Two separate temperature chambers, one for low temperature tests and another for high temperature tests, were constructed to house the loading apparatus with the specimen in place. The high temperature was attained with electric heating coils whereas the low temperature was attained with liquid nitrogen. A temperature controller and several temperature sensing probes located at various points in the chamber were used to achieve repeatable test temperatures. One of these probes was attached to the specimen surface in the test zone. Tests at high temperature were conducted at a specimen surface temperature of 366 K (199°F) whereas the tests at low temperature were conducted at 223 K (-59°F). The temperature variation in the vicinity of the specimen was within a degree Kelvin of the desired surface temperature.

Static bending loads were applied to the specimens through a specially built four-point loading apparatus. The tensile or the compressive loads were applied through a whiffletree arrangement connected to a screw jack in the rear. Photographs of a typical specimen with the loading apparatus and the general test arrangement are shown in Figures 2 and 3. A load cell was built into the loading apparatus. The load and the resulting strains in the specimen were measured using standard strain gage techniques. Two strain gages, oriented to measure the longitudinal strains, were bonded to the specimen equidistantly (2.5 cm from the center) from the geometric center of the test section. The ultimate load and the corresponding strains were determined using undamaged specimens. With the results of earlier tests in the background (4), the specimens were loaded and impacted by releasing the projectile to assess the damage tolerance of the specimens. Depending on the magnitude of the initial load (pre-load) and the projectile kinetic energy, the specimen either survived or failed catastrophically. Those specimens that survived the impact were tested for residual strength. In the high- and low-temperature tests, the thermally induced strains on the specimens and the thermal loads on the loading frame were measured prior to the initiation of the test

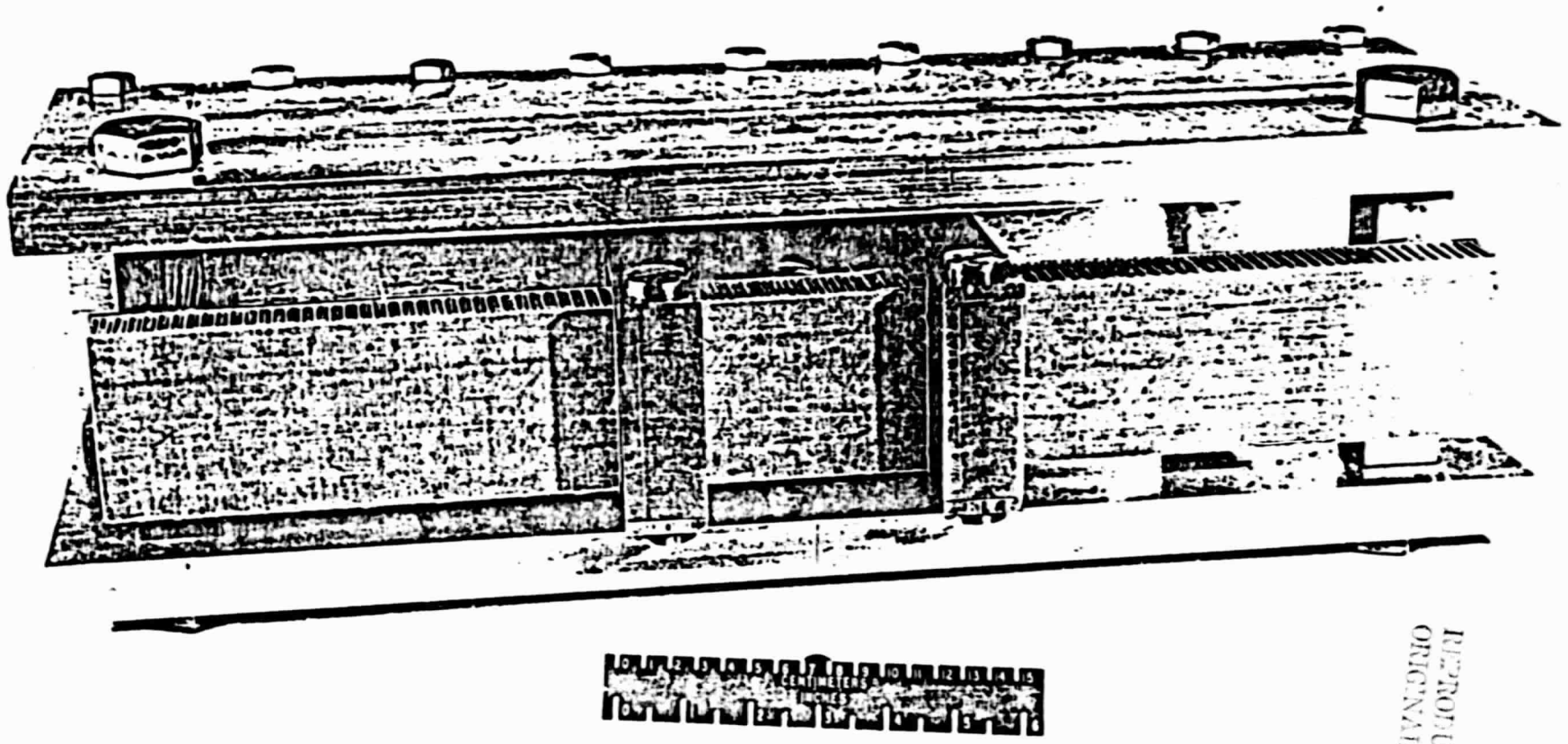

Figure 2. Typical Specimen with the Loading Frame (Compression Mode).

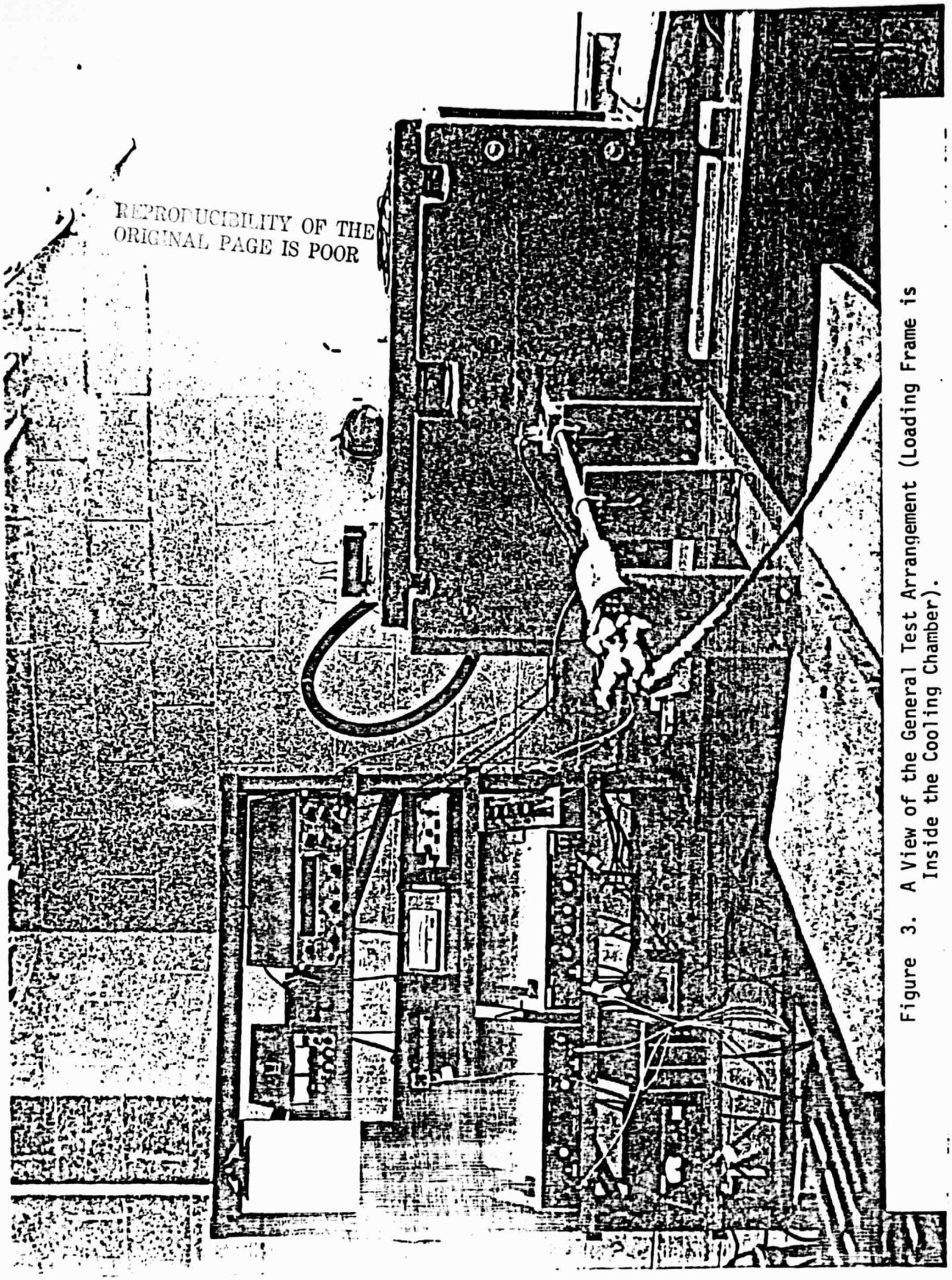

Figure 3. A View of the General Test Arrangement (Loading Frame is Inside the Cooling Chamber).

program and were found to be insignificant as compared to the applied loads and the strains. In actual testing, the strain gages were balanced after the specimen has achieved a steady state surface temperature.

Following Rhodes (3), the term failure threshold, used in subsequent sections, is defined as the lowest static load which precipitated catastrophic failure in the face sheet of a sandwich beam specimen at a given impact energy. The stress ratio, σ/σ_{ult}, used in this paper is defined as the ratio of the stress in the specimen prior to impact or the residual strength of the specimen to the ultimate strength of the virgin (undamaged) specimen.

RESULTS AND ANALYSES

The results of tests conducted with the eleven different laminates are shown in tabular forms. The theoretical modulii of the laminates in the spanwise direction of the sandwich beam were calculated using the usual laminate analyses. The experimental modulii were obtained from the stress-strain diagrams of the laminates. The basis used in the calculation of the modulii from the test results is shown in Figure 4. In general, a majority of the laminates tested have exhibited linear and slightly nonlinear behavior (Table I) under tensile- and compressive-loads, respectively. In the case of nonlinear behavior, these modulii as shown were calculated using the initial tangent modulus concept. The theoretical and the experimentally evaluated modulii for most of the laminates as shown in tables are in good agreement. The ultimate strength values were obtained from testing the undamaged specimens. Various laminate properties are shown in Tables II to V. The Tables II and IV have the properties of the tension- and the compression-loaded laminates, respectively, in SI system (Metric) whereas the Tables III and V have the corresponding properties in U.S. customary units. The residual strength of the impact-damaged test coupons as shown in Table VI is expressed as a percent of its ultimate strength. The failure threshold curves for the various

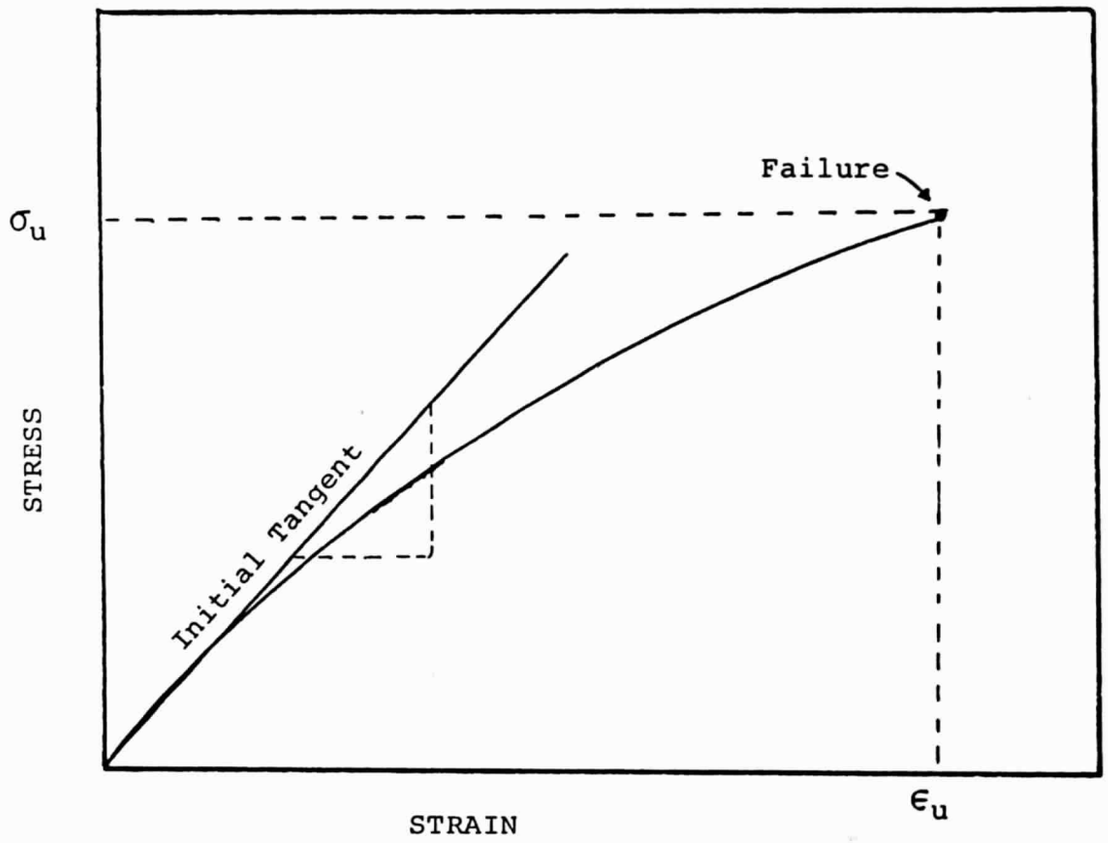

Figure 4. Basis in Calculating the two Modulii (Table I)

TABLE I. LAMINATE MODULII BASED ON LINEAR AND NONLINEAR σ-ε BEHAVIOR

Series Number	Material	Orientation	Tension Modulus			Compression Modulus		
			Theory	Experiment		Theory	Experiment	
			GPa(msi)	(Slope of Ini. Tgt) GPa(msi)	(σ_u/ε_u) GPa(msi)	GPa(msi)	(Slope of Ini. Tgt) GPa(msi)	(σ_u/ε_u) GPa(msi)
1	T300/5208	$(0_8)_T$	147(21.3)	167(24.2)	167(24.2)	131(19.0)	140(20.2)*	134(19.5)*
2	T300/5208	$(\pm 45, 0_4, 90)_s$	96(13.9)	95(13.7)	95(13.7)	87(12.6)	89(13.0)*	75(10.9)*
3	T300/5208	$(\pm 45_{\pm} 45, 0_2)_s$	64(9.3)	65(9.4)	65(9.4)	59(8.5)	65(9.4)*	60(8.7)*
4	T300/5208	$(\pm 45, 0_4)_s$	106(15.4)	109(15.8)	109(15.8)	95(13.8)	103(14.9)*	85(12.4)*
5	T300/5208	$(90, \pm 45, 0)_s$	58(8.4)	57(8.3)	57(8.3)	53(7.7)	56(8.2)*	54(7.9)*
6	T300/5208	$(\pm 45, 90, 0)_s$	58(8.4)	61(8.9)*	57(8.3)*	53(7.7)	57(8.2)*	50(7.3)*
7	Kev/5208, T300/5208	$(0_K, 90_G, 0_G)_s$	74(10.7)	82(11.8)	82(11.8)	74(10.7)	82(11.9)	82(11.9)
8	T300/5209	$(90, \pm 45, 0)_s$	56(8.1)	64(9.3)	64(9.3)	56(8.1)	60(8.7)*	52(7.6)*
9	T300/934	$(90, \pm 45, 0)_s$	51(7.5)	68(9.9)*	62(9.0)*	55(8.0)	55(8.0)*	49(7.1)*
10	Boron/5505	$(90, \pm 45, 0)_s$	81(11.8)	76(11.1)*	73(10.4)*	87(12.6)	86(12.4)*	79(11.5)*
11	Boron/5505 T300/5208	$(0_B, 90_G, 0_G)_s$	123(17.8)	137(19.9)*	107(15.5)*	121(17.5)	123(17.8)*	111(16.1)*

*Nonlinear stress-strain (σ-ε) behavior.

TABLE II. PROPERTIES OF THE LAMINATES IN TENSION

Series Number	Material	Orientation	Density kg/m^3	Strength (expt) GPa	Modulus (theory) GPa	Modulus (expt) GPa	Strain	Specific strength MN-m/kg	Specific Modulus (theory) MN-m/kg	Specific Modulus (expt) MN-m/kg
1	T300/5208	$(0_8)_T$	1520	1.67	147	167	0.010	1.10	97	110
2	T300/5208	$(\pm 45, 0_4, 90)_s$	1520	1.04	96	95	0.011	0.68	63	62
3	T300/5208	$(\pm 45, \pm 45, 0_2)_s$	1520	0.71	64	65	0.011	0.47	42	42
4	T300/5208	$(\pm 45, 0_4)_s$	1520	1.09	106	109	0.010	0.72	70	72
5	T300/5208	$(90, \pm 45, 0)_s$	1520	0.63	58	57	0.011	0.41	38	38
6	T300/5208	$(\pm 45, 90, 0)_s$	1520	0.57	58	61	0.010	0.38	38	38
7	Kev/5208, T300/5208	$(0_K, 90_G, 0_G)_s$	1473	0.82	74	82	0.010	0.55	50	55
8	T300/5209	$(90, \pm 45, 0)_s$	1520	0.64	56	64	0.010	0.42	37	42
9	T300/934	$(90, \pm 45, 0)_s$	1578	0.68	51	68	0.011	0.43	33	43
10	Boron/5505	$(90, \pm 45, 0)_s$	2020	0.51	81	76	0.007	0.25	40	38
11	Boron/5505 T300/5208	$(0_B, 90_G, 0_G)_s$	1687	0.64	123	137	0.006	0.38	73	81

TABLE III. PROPERTIES OF THE LAMINATES IN TENSION

Series Number	Material	Orientation	Density lb/in^3	Strength (expt) ksi	Modulus (theory) msi	Modulus (expt) msi	Strain	Specific strength $in.(10^6)$	Specific Modulus (theory) $in.(10^6)$	Specific Modulus (expt) $in.(10^6)$
1	T300/5208	$(0_8)_T$	.055	242	21.3	24.2	0.010	4.40	387	440
2	T300/5208	$(\pm 45, 0_4, 90)_s$	.055	151	13.9	13.7	0.011	2.75	253	250
3	T300/5208	$(\pm 45, \mp 45, 0_2)_s$	.055	103	9.3	9.4	0.011	1.87	169	170
4	T300/5208	$(\pm 45, 0_4)_s$	.055	158	15.4	15.8	0.010	2.87	279	287
5	T300/5208	$(90, \pm 45, 0)_s$	.055	91	8.4	8.3	0.011	1.65	153	150
6	T300/5208	$(\pm 45, 90, 0)_s$	.055	83	8.4	8.9	0.010	1.51	153	161
7	Kev/5208, T300/5208	$(0_K, 90_G, 0_G)$	.053	118	10.7	11.8	0.010	2.23	202	221
8	T300/5209	$(90, \pm 45, 0)$	.055	93	8.1	9.3	0.010	1.70	147	170
9	T300/934	$(90, \pm 45, 0)_s$	.057	99	7.5	9.9	0.011	1.74	131	174
10	Boron/5505	$(90, \pm 45, 0)_s$	.073	73	11.8	11.1	0.007	1.00	162	151
11	Boron/5505, T300/5208	$(0_B, 90_G, 0_G)_s$	.061	93	17.8	19.9	0.006	1.52	292	326

TABLE IV. PROPERTIES OF THE LAMINATES IN COMPRESSION

Series Number	Material	Orientation	Density kg/m^3	Strength (expt) GPa	Modulus (theory) GPa	Modulus (expt) GPa	Strain	Specific strength MN-m/kg	Specific Modulus (theory) MN-m/kg	Specific Modulus (expt) MN-m/kg
1	T300/5208	$(0_8)_T$	1520	1.34	131	140	0.010	0.88	86	92
2	T300/5208	$(\pm 45, 0_4, 90)_s$	1520	1.05	87	89	0.014	0.69	57	59
3	T300/5208	$(\pm 45, \pm 45, 0_2)_s$	1520	0.72	59	65	0.012	0.47	39	42
4	T300/5208	$(\pm 45, 0_4)_s$	1520	1.11	95	103	0.013	0.73	63	68
5	T300/5208	$(90, \pm 45, 0)_s$	1520	0.49	53	56	0.009	0.32	35	37
6	T300/5208	$(\pm 45, 90, 0)_s$	1520	0.60	53	57	0.012	0.39	35	37
7	Kev/5208, T300/5208	$(0_K, 90_G, 0_G)_s$	1473	0.82	74	82	0.010	0.56	50	56
8	T300/5209	$(90, \pm 45, 0)_s$	1520	0.57	56	60	0.011	0.38	37	40
9	T300/934	$(90, \pm 45, 0)_s$	1578	0.54	55	55	0.011	0.34	35	35
10	Boron/5505	$(90, \pm 45, 0)_s$	2020	0.87	87	86	0.011	0.43	57	43
11	Boron/5505, T300/5208	$(0_B, 90_G, 0_G)_s$	1687	1.33	121	123	0.012	0.79	72	73

TABLE V. PROPERTIES OF THE LAMINATES IN COMPRESSION

Series Number	Material	Orientation	Density lb/in^3	Strength (expt) ksi	Modulus (theory) msi	Modulus (expt) msi	Strain	Specific strength $in.(10^6)$	Specific Modulus (theory) $in.(10^6)$	Specific Modulus (expt) $in(10^6)$
1	T300/5208	$(0_8)_T$	.055	195	19.0	20.2	0.010	3.55	345	368
2	T300/5208	$(\pm 45, 0_4, 90)_s$	.055	152	12.6	13.0	0.014	2.76	229	236
3	T300/5208	$(\pm 45, \mp 45, 0_2)$	.055	104	8.5	9.4	0.012	1.89	155	170
4	T300/5208	$(\pm 45, 0_4)_s$	.055	161	13.8	14.9	0.013	2.93	251	271
5	T300/5208	$(90, \pm 45, 0)_s$	.055	71	7.7	8.2	0.009	1.29	140	148
6	T300/5208	$(\pm 45, 90, 0)_s$	.055	87	7.7	8.2	0.012	1.58	140	150
7	Kev/5208, T300/5208	$(0_K, 90_G, 0_G)_s$	.053	119	10.7	11.9	0.010	2.25	202	225
8	T300/5209	$(90, \pm 45, 0)_s$	.055	83	8.1	8.7	0.011	1.51	147	159
9	T300/934	$(90, \pm 45, 0)_s$	.057	78	8.0	8.0	0.011	1.37	140	141
10	Boron/5505	$(90, \pm 45, 0)_s$	.073	126	12.6	12.4	0.011	1.73	173	170
11	Boron/5505, T300/5208	$(0_B, 90_G, 0_G)_s$	.061	193	17.5	17.8	0.012	3.16	287	291

TABLE VI. ULTIMATE- AND RESIDUAL-STRENGTHS OF THE LAMINATES

Series Number	Material	Orientation	Plies	Tensile Strength σ_u, GPa (ksi)	Strength Retention (percent of σ_u)	Comp. Strength σ_u, GPa (ksi)	Strength Retention (percent of σ_u)
1	T300/5208	$(0_8)_T$	8	1.67 (242)	62	1.34 (195)	43
2	T300/5208	$(\pm45,0_4,90)_s$	14	1.04 (151)	45	1.04 (152)	32
3	T300/5208	$(\pm45,\pm45,0_2)_s$	12	0.71 (103)	62	0.72 (104)	37
4	T300/5208	$(\pm45,0_4)_s$	12	1.09 (158)	58	1.11 (161)	38
5	T300/5208	$(90,\pm45,0)_s$	8	0.64 (92)*	43	0.46 (66)*	57
				0.62 (90)#	47	0.52 (76)#	60
6	T300/5208	$(\pm45,90,0)_s$	8	0.57 (83)	55	0.60 (87)	51
7	Kev/5208, T300/5208	$(0_K,90_G,0_G)_s$	6	0.81 (117)*	50	-	-
				0.82 (119)#	50	0.82 (119)#	62
8	T300/5209	$(90,\pm45,0)_s$	8	0.64 (93)	55	0.57 (83)	45
9	T300/934	$(90,\pm45,0)_s$	8	0.68 (99)	33	0.54 (78)	38
10	Boron/5505	$(90,\pm45,0)_s$	8	0.51 (73)	70	0.87 (126)	65
11	Boron/5505, T300/5208	$(0_B,90_G,0_G)_s$	6	0.64 (93)	70	1.33 (193)	40

*Results at moderately high temperature (366 K)
#Results at moderately low temperature (223 K)

laminates tested in tension and compression are shown in Figures 5 and 6, respectively. It may be remarked that by properly selecting the combinations of the preload and the projectile kinetic energy, the failure threshold curves could be extended in both the directions. The extension of the curves to the left (Figs. 5 and 6) would eventually lead the stress ratio values to a point defined as $\sigma/\sigma_u = 1.0$ (4). The threshold curve extension to the right would tend to be asymptotic leading to the strength of the laminate with an induced flaw or hole (10).

The specific strengths and the corresponding specific modulii (theoretical) of all the laminates tested in tension and compression are shown in Figures 7 and 8, respectively. The undamaged specific strengths and the corresponding values at the failure threshold for each of the test laminates are also shown. The lines of constant strain are shown in the same figures for visualizing the ranges of strain for various test laminates. The specific-strength and -modulus of a typical aluminum (2024-T3) are also shown.

Tension-Loaded Laminates

Two of the laminates (Series 5 and 7) were tested at moderately low- and high-temperatures to assess the effect of the temperature on the strength carrying ability of these laminates as compared to the corresponding values at room temperature (4). Consequently, it has been observed (7) that the strength degradation in the presence of moderately low- and high-temperature was negligible. The strain at the failure threshold as shown in Fig. 7 is about one-half of the ultimate strain values for both these laminates.

Among the laminates tested, two of them (Series 7 and 11) were Kevlar-graphite and boron-graphite hybrids with epoxy matrices. The boron hybrid was found to have a higher specific modulus than the Kevlar hybrid (Fig. 7) whereas the reverse was true with respect to the specific strengths. The test data indicates

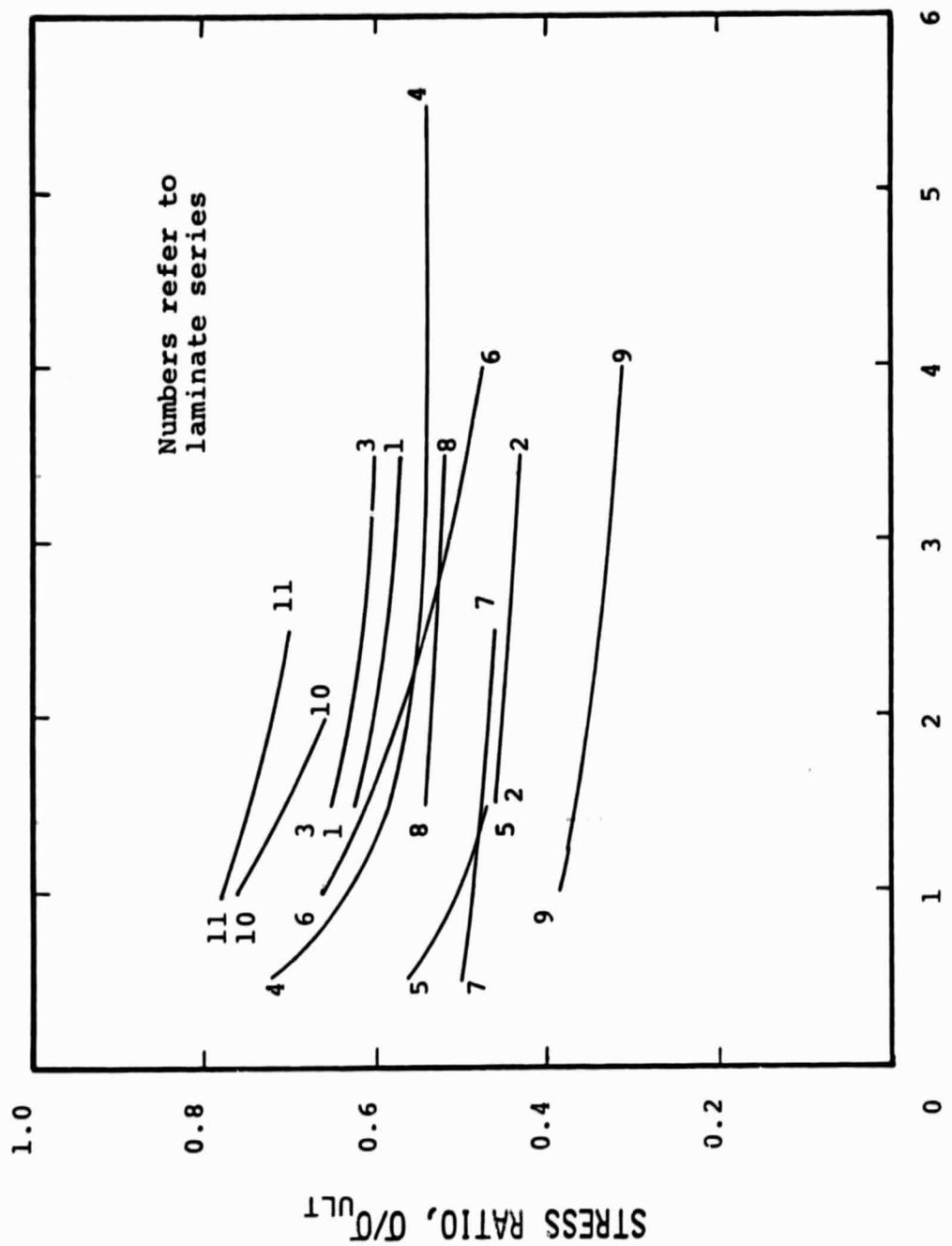

Figure 5. Failure Threshold Curves for Various Laminates (Tension)

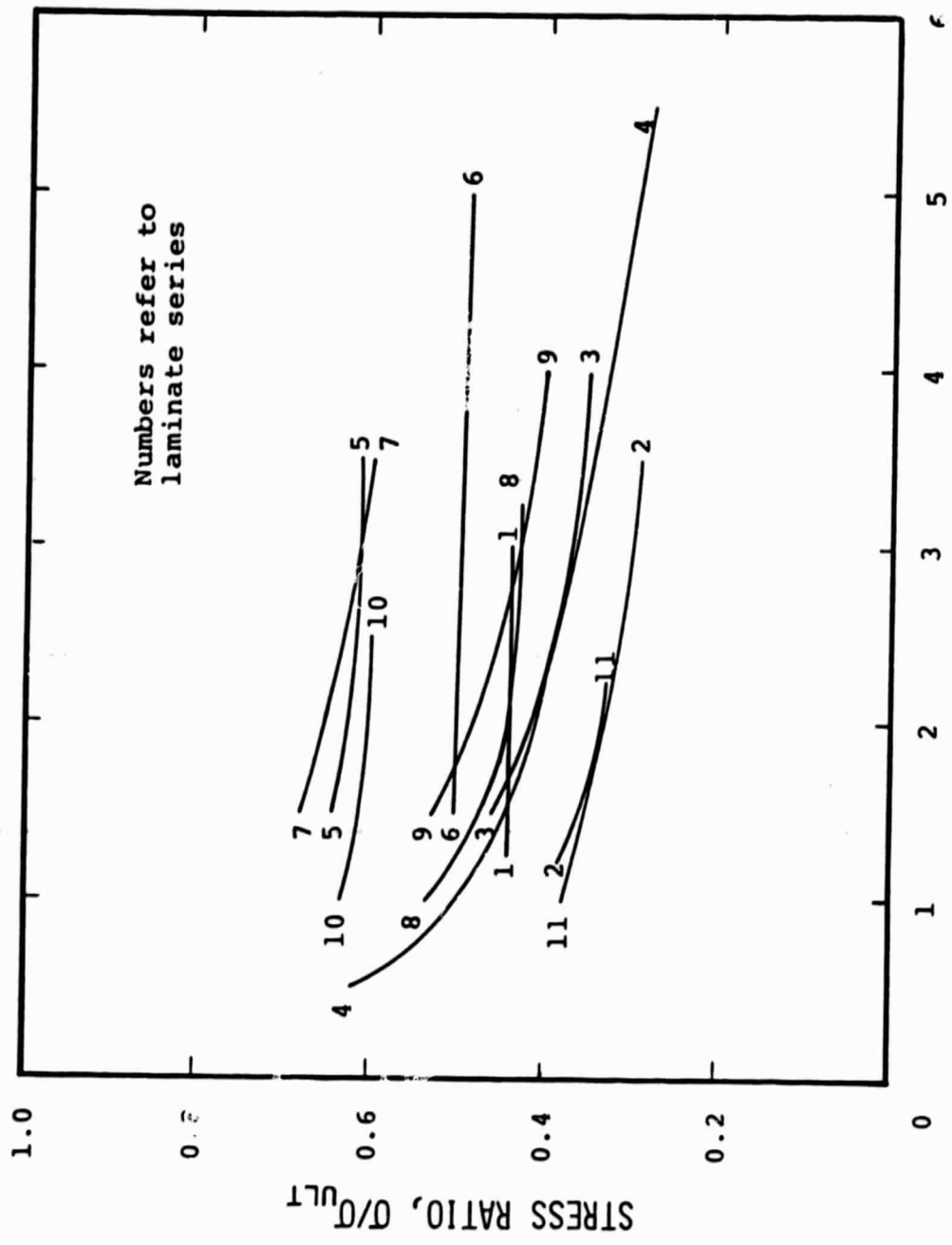

Figure 6. Failure Threshold Curves for Various Laminates (Compression)

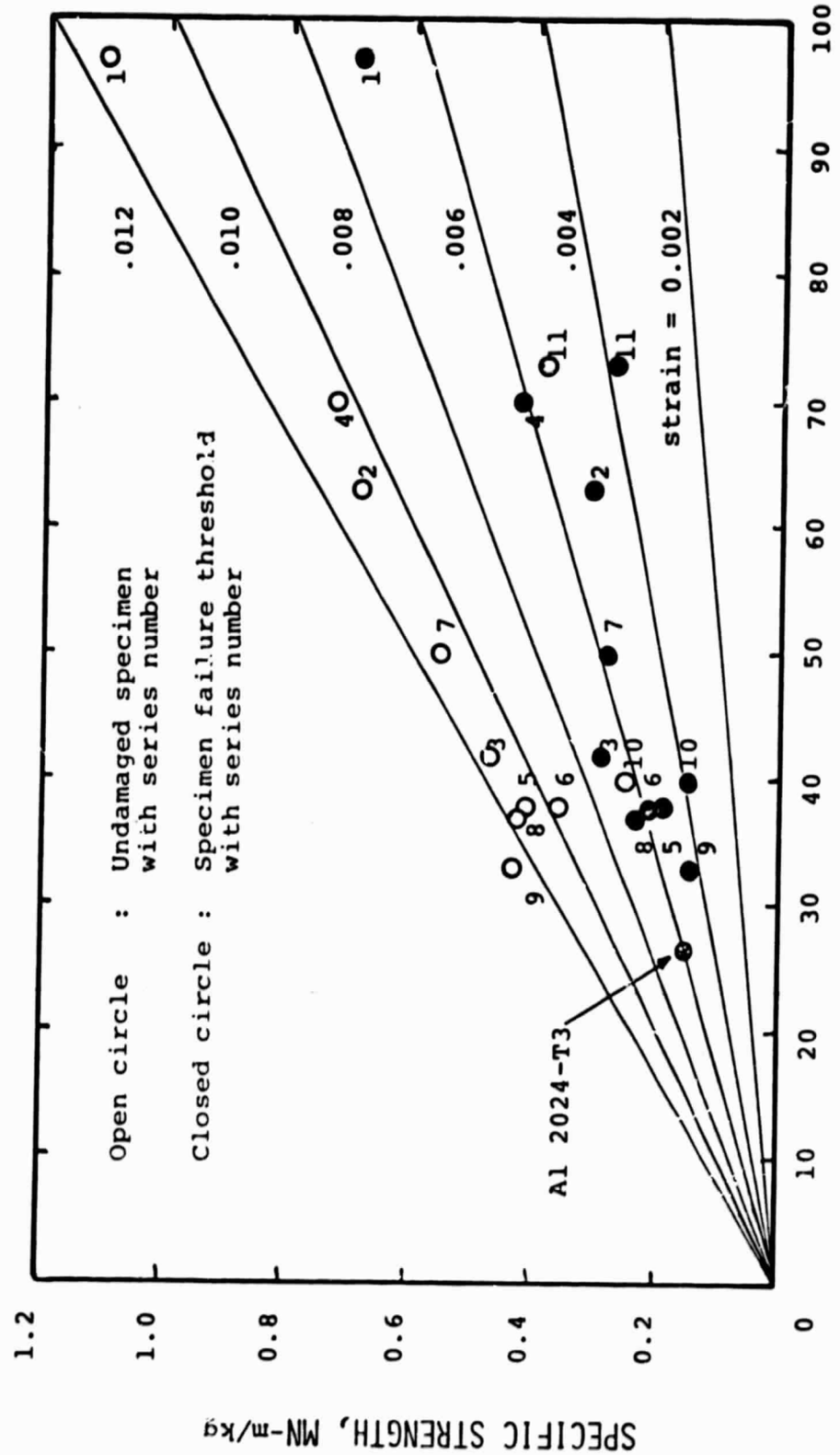

Figure 7. Specific Tensile Strength as a Function of Specific Tensile Modulus of Laminates in the Undamaged Condition and at the Failure Threshold

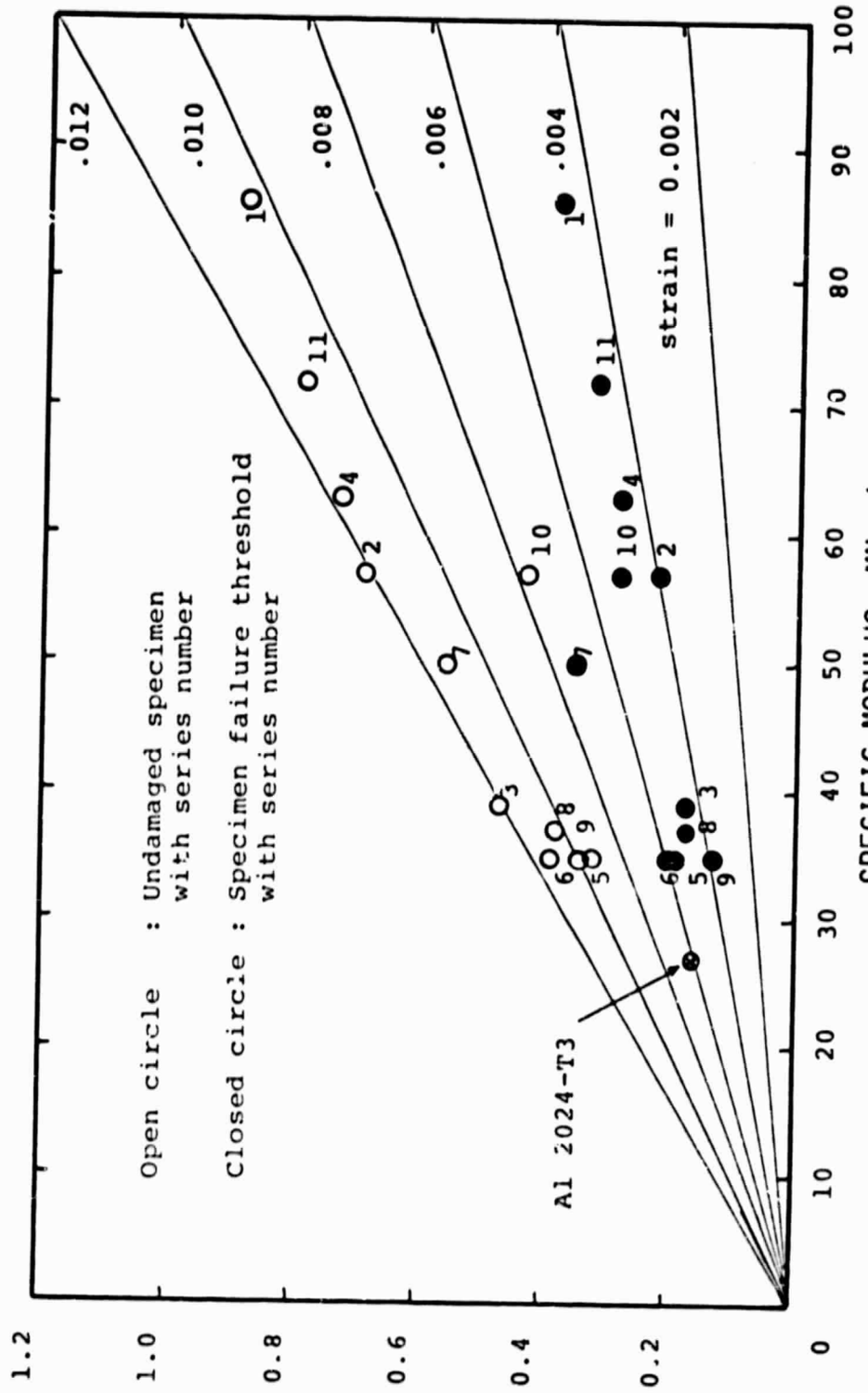

Figure 8. Specific Compressive Strength as a Function of Specific Compressive Modulus of Laminates in the Undamaged Condition and at the Failure Threshold

that the boron bybrid has better strength retention than the Kevlar hybrid (Fig. 5).

Some of the laminates (Series 1, 2 and 4) have 50% or more filament-controlled laminae (i.e., laminae with zero-degree lamina). The laminate with all zero-degree laminae (Series 1) has the highest specific-strength and -modulus (Fig. 7) followed by the laminates of Series 4 and 2. It may be noted that the laminates of Series 1, 4 and 2 have 8, 12 and 14 plies, respectively. However, the specific-strength and -modulus were found to decrease as the number of plies increases suggesting that increasing the thickness would not improve the undamaged strength and modulus of the laminates. The ultimate strains for all the above three laminates were found to be very close. The failure thresholds for the above laminates were also found to follow the same trend as the specific-strengths and -modulii (Fig. 5). The two additional cross plies in Series 2 have not proved to improve the properties when compared to the corresponding properties of Series 4.

The laminates in Series 5, 8 and 9 were identical with respect to the number of plies, the stacking sequence, the ply orientation, and the type of fibers. However, the matrices were different from one another. As shown in Fig. 7, there is no significant difference in the properties such as the specific-strength and -modulus among these laminates. The laminate (Series 9) with the matrix, Fiberite 934, has shown (Fig. 5) relatively poor impact resistance.

The orientation and the ply stacking sequence in Series 5 and 6 were reversed partially. The effect of this is not significant with respect to the strength- and stiffness-properties (Fig. 7). However, the presence of a 45-degree ply on the impact surface appears to have improved the impact resistance (Fig. 4). By observing the impact resistance of the laminates in Series 2, 3, 4 and 6, it may be seen (Fig. 5) that the laminate in Series 3 having the maximum number of 45-degree plies has relatively good impact resistance.

In general all the laminates, except the laminates in Series 10 and 11 having some or all boron plies, were observed to fail at strains in the range of 0.010 to 0.011. The corresponding strains at the failure threshold were from 0.005 to 0.007 (Fig. 7). The laminate with the Fiberite 934 matrix (Series 9) has shown the least impact resistance. The boron-based laminates (Series 10 and 11) appear to have poor specific strength and good impact resistance. Among the graphite/epoxy based laminate series, the unidirectional laminate (Series 1) and the laminate with the maximum number of angle (45-degree) plies (Series 3) have exhibited (Fig. 5) good impact resistance. The resistance to the projectile impact in most of the laminates tested appear to be better than 50% of their respective undamaged (or ultimate) strengths in the range of the impact energy levels considered.

Compression-Loaded Laminates

The specimens in Series 5 and 7 were also tested under compressive loads at moderately low- and high-temperatures. The failure thresholds for these laminates are shown in Fig. 6 and their specific-strength and -modulus values in Fig. 8. The compression test results were found to be similar to the tension test results, viz., the effect of the (low/high) temperature on the ability of the laminate to sustain loads was found to be insignificant when compared with the room temperature values. However, the two series of specimens were found to possess about 10% higher residual strength in compression (Fig. 6) than in tension (Fig. 5).

The two hybrid laminates in Series 7 and 11 were tested also in compression. The Kevlar hybrid has shown higher impact resistance than the boron hybrid. This trend is opposite to their behavior in tension (Figs. 5 and 6). With respect to the specific-strengths and -modulii of these laminates, the boron hybrid has shown better properties in compression than in tension. The tensile and the

compressive properties of the Kevlar hybrid were found to be the same whereas the boron hybrid has exhibited significant differences.

The laminates in Series 1, 2 and 4 having 50% or more filament-controlled laminae have exhibited a behavior in compression similar to those tested in tension, viz., the patterns of relative impact resistance, specific-strengths and -modulii among these laminates were found to be the same in both the tension and the compression tests. The magnitudes of these properties, however, were found to be lower in compression than in tension. The laminates in Series 2 (Fig. 6) were found to have the lowest impact resistance among all the laminate-series tested.

The specimens in Series 5, 8 and 9 have the same fibers but different matrices. The impact resistance of the laminates in Series 9 (with Fiberite 934) and Series 5 (with Rigidite 5208 matrix) has shown improvement in compression (Fig. 6) as compared to their corresponding resistance in tension (Fig. 5). On the other hand, the laminates in Series 8 (with Rigidite 5209 matrix) have exhibited relatively lower impact resistance in compression. The specific-strength and -modulus values for these three series were found to be slightly lower in compression than in tension.

The laminates of Series 5 and 6 have partially reversed orientation and stacking sequence. The Series 6 specimens having a 45-degree ply on the impact surface have not shown any improved impact resistance in compression when compared with the impact resistance of the laminates in Series 5 - this series has a cross-ply on the laminate (impact) surface. As indicated earlier, the reverse is true with the tension-loaded laminates. The specimens of Series 3 having a large number of 45-degree plies have not shown any improved impact resistance in compression whereas the reverse is true in tension tests (Fig. 5).

The results of all the compression tests conducted indicate that, in general, the laminates exhibit ultimate strains in the range of 0.010 to 0.012 with the

corresponding strains at the failure threshold in the range of 0.004 to 0.006. With a few exceptions, notably the laminates of Series 9 and 11, most of the laminates of the various series tested have exhibited higher specific-strengths and -modulii in tension than in compression. The impact resistance of the various series of the laminates tested shows that the tension-loaded laminates would sustain projectile impact loads slightly better than the corresponding laminates under compressive loads.

CONCLUSIONS

An experimental investigation was performed to evaluate the load carrying ability of various composite laminates subjected to low velocity projectile impact. Some of the laminates were tested at moderately low- and high-temperature to assess the effect of temperature on the various laminate properties including the impact resistance when compared to their corresponding room temperature properties. Based on the results of this investigation, the following conclusions can be drawn:

1. Trends in the impact failure threshold (asymptotic, monotonic, etc.) variations may be observed through the testing of a few laminates with a suitable combination of the preload and the kinetic energy of the impacting projectile.

2. Degradation in strength due to impact would depend not only on the type of laminate (fiber, matrix, stacking sequence and orientation) but also on the type of load (tensile or compressive) applied.

3. Moderately low- or high-temperatures have not affected the impact resistance of the laminates significantly.

4. Since the residual strengths of most of the laminates exceeded the strength values at the impact failure threshold, the failure threshold may be considered as a reasonable estimate of the strength of the impact-damaged laminates.

5. Since all the filament-controlled laminates exhibited ultimate strain values in a narrow range, these values may be considered as good indicators of the respective laminate strengths.

6. Laminates having 50% or more unidirectional laminae have shown better impact resistance under tensile loads than under compressive loads.

7. Laminates with more 45-degree plies closer to the impact surface were found to have higher resistance to impact in tension than in compression.

8. A majority of the laminate series have shown slightly higher specific-strengths and -modulii in the tension mode than in the compression.

9. Among all the laminates tested, the impact damage caused a strength degradation of the laminates from as low as 30 percent to as high as 70 percent of their respective ultimate strengths.

10. A majority of the laminates tested were found to have a slightly non-linear stress-strain behavior under compressive loads.

REFERENCES

1. Slepetz, J. M. et al., "Impact Damage Tolerance of Graphite/Epoxy Sandwich Panels" AMMRC TR 74-20, Sept. 1974.

2. Rhodes, M. D., "Low Velocity Impact on Composite Sandwich Structures," Presentation at the Second Air Force Conference on Fibrous Composites in Flight Vehicle Design, Dayton, Ohio, May 1974.

3. Rhodes, M. D., "Impact Fracture of Composite Sandwich Structures", Presentation at the ASME/AIAA/SAE 16th Structural Dynamics, and Materials Conference, Denver, Colorado, May 1975.

4. Rhodes, M. D., "Impact Tests on Fibrous Compostie Sandwich Structures", NASA-TM-78719, 1978.

5. Awerbuck, J., and Hahn, H. T., "Hard Object Impact Damage of Metal Matrix Composites", J. of Composite Materials, Vol. 10. July 1976.

6. Sharma, A. V., "Effect of Low Velcoity Projectile Impact on the Strength of Composite Sandwich Structures"; V Inter-American Conference on Materials Technology, Sao Paulo, Brazil, November 1978.

7. Sharma, A. V., "Effect of Temperature on Composite Sandwich Structures Subjected to Low Velocity Projectile Impact"; Winter Annual Meeting, The American Society of Mechanical Engineers, San Francisco, CA., December 1978.

8. Sharma, A. V., "Low Velocity Impact Tests on Fibrous Composite Sandwich Structures"; ASTM Specialist Symposium on 'Test Methods and Design Allowables for Fibrous Composites', Oct. 2-3, 1979, Dearborn, Michigan.

9. Sharma, A. V., "Damage Tolerance of Composite Structures Subjected to Projectile Impact"; 11th National SAMPE Technical Conference, Boston, MA., November 13-15, 1979.

10. Husman, G. E. et al., "Residual Strength Characterization of Laminated Composites Subjected to Impact Loading"; ASTM STP 568, 1975.